Evidence for shallow positron traps in a neutron-irradiated Al single crystal as studied with variable-energy positrons

P. J. Schultz,* K. G. Lynn, R. N. West,† C. L. Snead, Jr., and I. K. MacKenzie*

Brookhaven National Laboratory, Upton, New York 11973

R. W. Hendricks‡

Oak Ridge National Laboratory, Oak Ridge, Tennessee 37830

A monoenergetic (± 1 eV), variable-energy (0.5—4 keV) beam of positrons has been used to study the dependence on temperature (40—350 K) of positron diffusion out of a neutron-irradiated single crystal of Al. The results are interpreted in the context of a one-dimensional diffusion model which encompasses annihilations as well as trapping at voids and other microstructural defects in the bulk material by way of a removal rate κ_{eff} of positrons from freely diffusing states. κ_{eff} is found to have a slightly positive dependence on temperature above 125 K, as would be expected from previous measurements of the positron trapping rate into large voids. The data suggest a strongly negative dependence on temperatures below 125 K for κ_{eff}, indicating the presence of some additional phenomenon which we attribute to positron localization in shallow, presumably radiation-induced, traps in the crystal. The results of our analyses provide support for conclusions reached previously for neutron-irradiated Mo. During preliminary annealing treatments of the sample we found, by Auger-electron spectroscopy, that Si produced by neutron-induced transmutation migrated to the crystal surface. It is conjectured that redistribution of Si within the sample is responsible for a recovery stage previously observed in neutron-irradiated Al between 400 and 470 K.

I. INTRODUCTION

Recent positron studies[1,2] of neutron-irradiated metals containing voids have shown that the fraction of positrons which annihilate in the longest-lived states normally associated with positrons trapped at voids decreases significantly as the specimen temperature is lowered below ~200 K. Nieminen et al.[1] explained this effect, which was observed in aluminium, in terms of an intrinsic positron-void trapping rate that has a strong positive temperature dependence at low temperatures. Schultz et al.[2] studied neutron-irradiated molybdenum and found some evidence of a more complex picture. Specifically it was suggested that other defects produced by neutron irradiation in their samples provide shallow trapping centers from which the positrons can be thermally desorbed at relatively low temperature (below room temperature). The decreasing fraction of positrons in shallow traps for increasing temperature results in a corresponding increase in the fraction able to in-

teract with the voids. Which of these interpretations is most applicable is currently unresolved since neither of the studies in question could clearly resolve any of the potentially large number of other defect components in the irradiated specimens.

The possibility of shallow positron traps has been suggested in connection with positron trapping at grain boundaries,[3,4] defects generated in molybdenum by electron irradiation,[5] and dislocations in various metals.[6] A direct confirmation of their existence is not straightforward since the sensitivity of conventional studies of positron-trapping phenomena depends on the difference between the annihilation characteristics for the trapped and freely diffusing positron states which, in the case of shallow traps, would be expected to be relatively small.

A less conventional study of this problem is made possible by the development of slow-positron beams in ultrahigh-vacuum conditions[7−9] which permit a relatively direct measurement of the tem-

perature dependence of the positron diffusion length (L_+) in the near-surface ($\lesssim 1000$ Å) region. The diffusion length is

$$L_+ = (D_+ \tau_{\text{eff}})^{1/2} , \qquad (1)$$

where D_+ is the positron diffusion coefficient, and $\tau_{\text{eff}}^{-1} (= \kappa_{\text{eff}})$ is the total rate of removal of positrons from the freely diffusing states by annihilation and trapping before the positron diffuses back to the surface. D_+ is expected to exhibit a $T^{-1/2}$ dependence on temperature since the diffusion > 10 K is dominated by acoustical phonon scattering.[10-12] Thus, a measurement of the temperature dependence of L_+ provides, through the dependence of L_+ on κ_{eff}, a test of the two models for neutron-irradiated metals since each, in its simplest form, implies an opposite sense for the temperature dependence of κ_{eff} at low temperatures.

In this paper results are presented for a variable-energy positron beam study of the temperature dependence of L_+ ranging from 40 to 350 K in a neutron-irradiated single crystal of aluminum. The organization of the paper is as follows. Experimental details are given in Sec. II. In Sec. III the basic theory relating the data to the temperature dependence of L_+ are presented along with the preliminary data analysis. These results are discussed in Sec. IV where it is shown that the temperature dependence of L_+ changes dramatically at or around 125 K. In the higher-temperature domain the results are consistent with a D_+ varying as $T^{-1/2}$ and a κ_{eff} having a positive temperature dependence similar to that inferred from the results of more conventional positron studies of neutron-irradiated metals.[1,13,14] κ_{eff} has a strong negative dependence on temperature below 125 K, consistent with desorption of a significant fraction of positrons from shallow traps. A model describing a temperature-dependent competition between the probability of positron localization in shallow traps, in deeper traps including voids, or annihilation from the freely diffusing state provides a good representation of the data. As an aid to clarity and continuity the details of the model are included in an appendix where most of the theoretical results are derived.

II. EXPERIMENTAL

The Al single crystal used in this study was irradiated to a neutron fluence of approximately $1.2 \times 10^{21} n/\text{cm}^2$ ($E > 0.18$ MeV) in the Oak Ridge

High-Flux Isotope Reactor (HFIR). It was cut from the ingot labeled Al-3, as defined in Ref. 15, into a parallel-sided disk of diameter ~ 25 mm and thickness ~ 3 mm with axis roughly $12°$ off the $\langle 110 \rangle$ direction. Transmission electron microscopy (TEM) and small-angle neutron and x-ray studies (SANS and SAXS) were performed on various specimens from the same ingot.[15,16] These experiments found a void-size distribution with a mean void diameter of about 400 Å and a distribution with a full width at half maximum (FWHM) of ≤ 200 Å. Earlier bulk positron studies[17] also identified additional small vacancy clusters ($\sim 5 - 10$ vacancies) which appeared to be stable upon annealing to 620 K. The ^{28}Si produced by the $\text{Al}(n, \gamma)$ reaction was estimated to be 1000 at. ppm (Ref. 18) while the concentration of voids was found to be about 5×10^{14} cm^{-3}.[15] Theoretical calculations suggest that voids will not form without the presence of some stabilizing impurities.[19,20] Hendricks *et al.*[18] suggest that the surfaces of the voids may be covered by as much as two atomic layers of Si. This hypothesis has been strengthened by direct observations of a thick Si coating on voids in an Al alloy irradiated to higher fluence.[21]

The slow-positron apparatus used for the experiments has been described elsewhere.[22] It provides a collimated beam (diameter ~ 6 mm) of essentially monoenergetic positrons, tunable in energy from 10 to 5 keV (± 5.1 eV) in ultrahigh-vacuum conditions. The base pressure throughout the measurements was approximately 5×10^{-10} Torr. The Al crystal was mounted on the cold stage of a closed-cycle He refrigerator in such a way as to electrically isolate the specimen to 5 kV and to allow presentation to low-energy-electron diffraction (LEED) and Auger-electron spectroscopy (AES) optics, and to the positron beam. The sample could also be cleaned by Ar-ion sputtering and heated *in situ* by an electron gun. The sample temperature was monitored continuously with two Chromel-Alumel thermocouples which agreed to within 2 K.

Measurements of the energy spectrum of annihilation photons emerging from the sample and its immediate vicinity were made with a Ge(Li) detector which had a resolution ~ 1.4 keV FWHM at 477.6 keV. The measurements were made as a function of incident positron beam energy and sample temperature. A central issue is the determination of a positronium fraction (F) which is defined as the fraction of the implanted positrons

which are subsequently re-emitted from the surface of the crystal as positronium (Ps). F can be derived from the measured energy spectrum as is described more fully, together with the relationship between F and positron diffusion, in the next section. Each spectrum took about 30 sec to produce a statistical precision of $\sim 0.5\%$ in F.

III. BASIC THEORY AND DATA ANALYSIS

When a positron, initially of kinetic energy E, penetrates a metal surface it rapidly thermalizes ($t \sim 10$ psec) at a mean depth ranging, for example, from ~ 50 Å at 500 eV to ~ 800 Å at $E = 5$ keV.[23] Thereafter the positron diffuses through the metal eventually annihilating from its freely diffusing state, or from any of a variety of possible localized states, with characteristic lifetimes before annihilation ranging from ~ 90 to 500 psec.[24] These annihilations almost always result in the emission of two ~ 0.511-MeV γ rays at approximately 180° from each other. A low-energy ($E \lesssim 10$ keV) positron after thermalization may also diffuse back to the metal surface and there or nearby become involved in one or other of three main processes: (i) localization in a surface state with possible subsequent thermal desorption into the vacuum as Ps at sufficiently high sample temperatures[25,26]; (ii) direct reemission into the vacuum as a free positron if the positron work function (ϕ_+) is negative[27,28]; (iii) direct reemission as Ps without apparent energy loss.[7-9]

Ps is an electron-positron bound state, of binding energy 6.8 eV in vacuum, which is formed by the pickup of an electron as the positron moves through the metal-vacuum interface.[7-9,29] Ps exists in the vacuum in either the triplet ($^3S_1$) or singlet ($^1S_0$) ground states from which it decays predominantly by the emission of three ($\tau_1 = 0.140$ μsec) or two ($\tau_0 = 0.125$ nsec) γ rays, respectively. The γ-ray energy spectrum from para-Ps ($^1S_0$) decays is essentially the same as that for the annihilation of positrons in bulk metal (i.e., a Doppler-broadened line at 0.511 MeV). In contrast the energy spectrum from ortho-Ps $^3S_1$ annihilation is continuous from 0 to 0.511 MeV, increasing in intensity as a function of monotonically increasing energy.[30] In our experiments the detector geometry is such that the measured γ-ray energy spectrum includes contributions from positron annihilation in the bulk sample, its surface regions, and the surrounding vacuum. Since both theory[31] and experi-

ment agree that Ps does not exist in bulk metal,[32] the relative contribution of ortho-Ps to the measured energy spectrum provides a measure of the fraction of implanted positrons that have diffused back to the metal surface.

The calculation of a Ps fraction F is based on the ratio $R_F = (T_F - P_F)/P_F$,[7,8] where T_F is the total number of counts in the spectrum and P_F is the counts in the 511-keV peak (500−520 keV):

$$F = \left[1 + \frac{P_1}{P_0} \left[\frac{R_1 - R_F}{R_F - R_0} \right] \right]^{-1}, \tag{2}$$

where the subscripts 1 and 0 refer to the situations where 100% and 0% of the implanted positrons are reemitted as Ps atoms, respectively.[23] The determination of R_0 and R_1 is relatively straightforward. R_0 is usually obtained by extrapolating curves for T_F and P_F to high incident positron energy and high sample temperature while R_1 is similarly obtained by extrapolation of T_F and P_F to $E = 0$ at high sample temperature (see Ref. 33 and discussions therein). Alternatively R_0 can be obtained by a measurement on a crystal with excessive surface damage (such as after sputtering) or impurity overlayers (such as amorphous Al_xO_y) since both conditions inhibit Ps emission by greatly enhancing the probability of positron trapping at the surface. The values for R_1 and R_0 depend on many factors including the sample and detector geometry and the detailed response of the detector to γ rays of different energy. Since R_1 and R_0 are ratios they do not depend on the integrated positron flux. P_1 and P_0 on the other hand, being numbers, must refer to identical flux conditions for Eq. (2) to be valid. Ideally, all these asymptotic values should be determined with the same specimen and in the same experimental run as the other F measurements. This possibility was precluded for our experiments by the need to preserve the defects in the sample. Accordingly, the values of R_1, R_0, and P_1/P_0 used in our analysis of the present data were taken from earlier and subsequent measurements on other Al samples. Our justification for this step is that the values in question, $R_0 = 3.6 \pm 0.2$, $R_1 = 13 \pm 1$, and $P_1/P_0 = 0.43$, have been stable parameters of the system over a period of a few months.

Figure 1 shows values for F that were obtained at each sample temperature for 15 different values of incident positron energy ranging from 0.5 to 4.0 keV in steps of 250 eV. Each scan of the specimen at constant temperature was then analyzed using the Appendix equation (A6), or
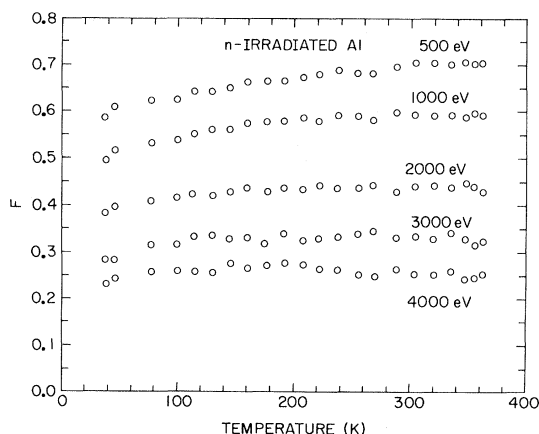
FIG. 1. The fraction (F) of incident positrons that emerge as positronium (Ps) is shown as a function of temperature and incident positron energy for an n-irradiated single crystal of Al. A total of 15 different energies were done at each temperature, ranging from 500 to 4000 eV. F is obtained from the experimental data according to Eq. (2). The required constants are $P_1/P_0 = 0.43$, $R_0 = 3.6 \pm 0.2$, $R_1 = 13 \pm 1$.

$$F = F_0 [1 + (E/E_0)^n]^{-1} . \tag{3}$$

Each analysis involved a nonlinear weighted fit to Eq. (3) from which we extracted a mean value for n. The quantity E_0 is the energy needed to implant the positrons far enough into the sample so that only one-half of them can diffuse back to the surface before annihilation in the free state or traps. E_0 depends only on bulk properties since it indicates the effect of implant depth on the fraction of positrons that diffuse back to the sample surface. The best value for n for both the data sets presented in the next section was $n = 1.34$. The data were then refitted using this value of n. In high-purity well-annealed single crystals of Al at room temperature E_0 (for a definition see Appendix Sec. 1) has been found to be ~ 3000 eV, F_0 about 0.5 to 0.6, and $n \sim 1.6$.[33] It has also been found that n decreased when deep traps were present in the bulk crystal.[33] The discussion in Sec. I of the Appendix would suggest that the reasons may be complex.

It is worth pointing out that the deduced value of E_0 and hence a relative measure of L_+ (Appendix Sec. 1) is not dependent on the surface conditions of the crystal under study. Specifically, since the branching ration to Ps (relative to other surface processes) for a fully thermalized positron that diffuses back to the surface cannot be a function of

E, then the only requirement for a measurement of E_0 is that there must be a finite Ps fraction. If the temperature changes are small during the measurement of each complete set of incident energies, then quantities that are potentially subject to temperature changes (such as the positron work function, absorption of trace impurities on the surface, or the absolute branching ratio to Ps) do not affect E_0. It should be noted, however, that the sensitivity to changes in F vs E (hence the accuracy of the value found for E_0) is dependent on the magnitude of F, as well as the number (and maximum value) of incident energies measured for each temperature.

Figure 2 shows one set of F values versus incident energy and the fit of Eq. 3 to the data. Such fits yield the values of $E_0(T)$ that are shown in Fig. 3. As explained in the Appendix of this paper,

$$E_0^n = \frac{1}{A} (D_+ / \kappa_{\text{eff}})^{1/2} , \tag{4}$$

where D_+ is the positron diffusion coefficient in freely diffusing state and κ_{eff} is the total rate of removal of positrons from those states by annihilation and trapping. Above ~ 150 K, E_0 decreases with increasing specimen temperature as is the case in well-annealed pure metal crystals.[12,34] Below 150 K the behavior is quite different and could be ascribed to an equally dramatic change in the temperature dependence of either (or both) D_+ or κ_{eff}.

Bergersen *et al.*[12] represent D_+ through a total
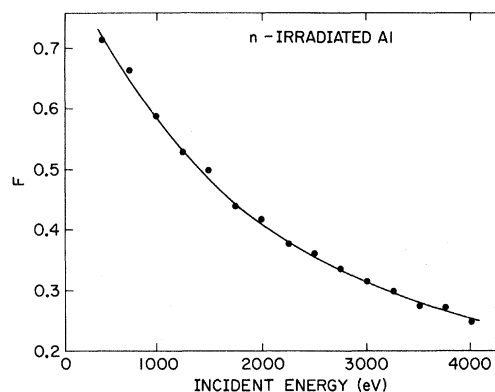
FIG. 2. The Ps fraction (F) is shown as a function of incident positron energy, together with the fit of Eq. (3) to obtain E_0. This set of data was taken with a sample temperature of ~ 265 K. The goodness-of-fit for data sets at all temperatures was similar to that for the results shown.
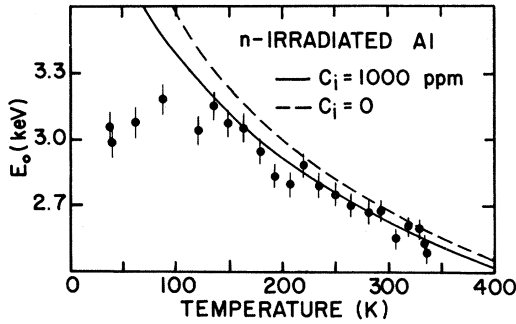
FIG. 3. E_0 is shown as a function of temperature for data from the third run, together with the theoretical predictions (neglecting shallow traps) described in the text. The dashed curve was calculated assuming diffusion with no impurity scattering, and the solid curve allowed for an impurity concentration of 1000 at. ppm. Other relevant parameters are listed in Table I. The curves indicate that the behavior of E_0 at low temperatures cannot be adequately described by impurity scattering.

relaxation time for scattering (τ):

$$D_+ = \frac{k_B T}{m^*}\tau , \qquad (5)$$

where m^* is the positron effective mass. The contributions to τ for positron scattering by conduction electrons (τ_e), by acoustic phonons (τ_{ph}), and by impurities (τ_i) are

$$\frac{1}{\tau} = \frac{1}{\tau_e} + \frac{1}{\tau_{ph}} + \frac{1}{\tau_i} , \qquad (6)$$

where

$$\tau_e = \frac{4m\hbar\epsilon_F}{\pi m^*(k_B T)} ,$$

$$\tau_{ph} = \frac{4\hbar^4 B}{E_d^2(m^* k_B T)^{3/2}\sqrt{3}} , \qquad (7)$$

$$\tau_i = \frac{\sqrt{3}\hbar^4}{4C_i m^{*3/2}R_a^3(V_{0I}-V_{0H})^2(k_B T)^{1/2}} .$$

In the above, m is the electron rest mass, ϵ_F the Fermi energy, B the bulk modulus, C_i the impurity concentration, R_a the impurity "cell" size, $V_{0I}-V_{0H}$ the host-impurity pseudopotential difference, and E_d is the deformation potential.

The concept of a deformation potential was first applied to the problem of electron scattering from acoustic phonons in semiconductors.[35,36] It is, quite simply, a pseudopotential representation of the band shifts invoked by a gradual distortion of

the lattice. When a slowly varying electrostatic potential is superimposed on the periodic potential of the crystal lattice, it is often a good approximation to neglect the latter for purposes of calculating electron (or positron) motion. In such calculations, one would substitute an appropriate effective mass for the electron's mass. Bardeen and Shockley[36] have shown that the long-wavelength disturbance of the energy bands produced by acoustical phonons can be separated from approximate, spherical bands in an analogous manner. They label slowly varying, effective potentials of this sort "deformation potentials." The above solution for τ_{ph} was taken from a calculation made in the deformation potential limit.[37] An approximate value for E_d is $(\frac{2}{3})\epsilon_F$, which is valid for the $q=0$ extremum of the phonon dispersion relation.

τ_{ph}^{-1} is roughly 100 times larger than τ_e^{-1} (at 300 K) for most metals,[12] and therefore is the dominant factor for D_+ in Eq. (1). For most situations, impurity scattering does not contribute significantly until very low temperatures (<10 K). Figure 3 shows the effect of relatively high concentrations of impurities on D_+ for Al, as reflected in the best fit of Eq. (4) to the results for E_0. Most of the parameters used to generate the curves in Fig. 3 are listed in Table I. The effective mass m^* was arbitrarily adjusted to $\sim 1.35m_0$ in order that D_+ (300 K) be approximately 0.76 cm^2/sec to agree with recent results for thin polycrystalline films of Al.[38] This is somewhat smaller than the value $m^* \sim 1.5m_0$ obtained by angular-correlation studies.[39] The Fermi energy, $\epsilon_F \sim 11.63$ eV, was taken from Ref. 40. E_0 is shown as a function of temperature in Fig. 3 for two cases. The first assumes there are no impurities, and for the second, $C_i = 1000$ at. ppm. The latter curve was calculated using a pseudopotential difference $V_{0I}-V_{0H}=0.1$ Ry. A value of $V_{0I}-V_{0H}=0.16$ Ry represents Li in Al, which has one of the highest pseudopotential differences.[12]

IV. DISCUSSION OF RESULTS

The results of four separate experimental runs on Al are reported, each consisting of sputter cleaning at room temperature, a 1-h anneal to remove surface damage caused by the sputtering, and the collection of data while the temperature was decreased from the annealing temperature to 40 K. For the first run, the specimen was sputtered in 5×10^{-5} Torr Ar at an energy of 1 keV (~ 10 μA

TABLE I. Parameters are listed for the theoretical curves in Figs. 3—5. The numbers in parentheses following some parameter values refer to the source from which they were taken. Parameters without reference were adjusted for best fit to the data, unless otherwise noted in the text or previously referenced in the table. The asterisks to the left of the table indicate those parameters which were allowed to float in the nonlinear fitting routine. (NA denotes values not applicable.)

Parameter	Symbol	Value Figure 3 (dashed)	Figure 3 (solid)	Figures 4 and 5 third run	fourth run
Diffusion coefficient					
impurity concentration (ppm)	C_i	0	1000 (18)	1000	1000
Fermi energy (eV)	ϵ_F	11.63 (40)	11.63	11.63	11.63
deformation potential (Ry)	E_d	0.63 (12)	0.63	0.63	0.63
bulk modulus (N/m^2)	B	7.22×10^{10} (12)	7.22×10^{10}	7.22×10^{10}	7.22×10^{10}
positron effective mass $(\times m_0)$	m^*	1.348	1.348	1.348	1.348
impurity "cell" size (Å)	R_a	NA	3	3	3
host-impurity pseudopotential difference (Ry)	$V_{0I}-V_{0H}$	NA	0.1	0.1	0.1
Others					
free annihilation rate (sec^{-1})	λ_1	6.135×10^9 (45)	6.135×10^9	6.135×10^9	6.135×10^9
shallow-trap annihilation rate (sec^{-1})	λ_2	NA	NA	6.135×10^9	6.135×10^9
*void trapping rate (sec^{-1})	κ_α	1.56×10^{10}	1.56×10^{10}	1.56×10^{10}	2.73×10^{10}
*void trapping $(\text{sec}^{-1}\text{K}^{-1})$	κ_β	3×10^7	3×10^7	3×10^7	1.7×10^7
*desorption temperature (K)	T_2	NA	NA	159	153
*~relative proportion of shallow traps to free states	N_{ST}/N_C	0	0	0.04	0.12
*λ_2 rate into shallow traps	λ_2/κ_{12}	NA	NA	0.26	0.10
relates E_0 to depth $(\text{Å}/kV^n)$	A	130	130	130	130
(see text)	n	1.34	1.34	1.34	1.34

sample current) for several hours, then annealed at 375 K; annealing studies of neutron-irradiated Al (Refs. 13 and 16) have shown that the voids induced by neutron irradiation do not begin to anneal out until temperatures above about 425 K. Unusually low values of the Ps fraction were found after this procedure [$F < 15\%$ with 500-eV incident positrons, compared with about 50% for clean Al (Ref. 33)]. The low values were attributed in part to a significant Al_xO_y overlayer for which evidence was found by AES. Amorphous Al_xO_y is known to inhibit Ps formation at room temperature most likely by trapping positrons.[33] The F values were sufficiently low to decrease the sensitivity to any fit for E_0 beyond the level where reasonable systematics could be extracted. It is, nevertheless, significant, with reference to observations that follow, that the AES measurements indicated no sign of surface impurities except Al_xO_y with annealing at 375 K.

The second run consisted of a cleaning and annealing procedure identical to the first, with the exception that the energy of the Ar-ion beam was increased to 1.5 keV. In this case AES measurements demonstrated that the surface was free of any contaminant, but excessive trapping was still observed ($F < 25\%$ at $E = 500$ eV). It was concluded that the annealing temperature (375 K) was too low to completely recover the damage caused by sputtering in one hour. Low values of E_0 (~ 700 eV), F_0 (~ 0.4) and, n (~ 0.8) also supported this conclusion.

By raising the annealing temperature to 425 K for both the third and fourth data sets it was possible to both clean and recover the surface. AES for both these runs indicated that the surface was relatively clean, showing traces of C and O ($<< 1\%$ of the surface; Ref. 41) and a reasonably significant Si peak ($\sim 8\%$ of the surface). It is this evidence of Si (roughly the same amount both times) that revealed the significance of the first two runs. In the dynamic annealing studies of Alam et al.,[13] there is the suggestion of a recovery stage between 400 and 470 K for which there was

no obvious explanation. We believe that the absence of Si on the surface in the first two runs (375 K), and its presence in the second two (425 K) indicates that the observed recovery stage[13] is accompanied by the migration of Si. As mentioned previously, Si probably coats the void surfaces as well as being distributed throughout the bulk lattice after neutron-irradiation, prior to annealing.[18]

The data for runs three and four are very similar. Both lead to a dependence of E_0 on temperature above ~ 125 K that is consistent with the scattering mechanisms described in the preceding section. The solid curve in Fig. 3 indicates that the weakening of the dependence of D_+ on tem-

perature caused by impurity scattering is not sufficient to explain the low-temperature (< 125 K) results.

The introduction of an entirely different mechanism affecting the diffusion of the positron is demonstrated most strikingly by a plot of the effective free positron removal rate κ_{eff} versus temperature, as shown for both the third and fourth data sets in Fig. 4. κ_{eff} is obtained by factoring $D_+(T)$, n, and A out of the E_0 data [Eq. (4)]. The solid curves in Fig. 4 represent the best fits to the trapping-model equation (A11), Appendix Sec. 3, rewritten as

$$\kappa_{eff}(T)=\lambda_1+\kappa_\alpha+\kappa_\beta T+\lambda_2\left[\frac{\lambda_2}{\kappa_{12}}+\frac{N_c}{N_0}\left[\frac{T}{300}\right]^{3/2}\exp(-T_0/T)\right]^{-1}. \tag{8}$$

Here
$$N_c=2(2\pi m^* k_B 300/h^2)^{3/2}=2.5\times10^{19}(m^*/m_0)^{3/2}$$
(Ref. 42), $T_0=\epsilon_0/k_B$, κ_α, and κ_β represent the total trapping rates for all types of deep traps, and λ_1, λ_2, and λ_{12} are all regarded as temperature independent. The parameters for the two theoretical curves are listed in Table I.

There are several results from Fig. 4 that are consistent with earlier findings. One difference between the two sets of data in Fig. 4 is the slope above ~ 125 K (see κ_β in Table I). In the third run there is only a weak positive dependence on temperature that can be attributed to the void (and other "deep" traps) trapping rate. By the fourth run this is weakened further. In positron-lifetime and Doppler-broadening measurements performed in neutron-irradiated Mo,[2] a similar reduction in the dependence of κ_{13} ($\equiv\kappa_\alpha+\kappa_\beta T$) on temperature was observed after partial recovery of the specimen. Since the sputter-cleaning of the Al between runs three and four necessitated an additional anneal (425 K), we attribute this effect to the recovery of some of the deeper traps in the crystal which contribute to the dependence of κ_{13} on temperature. This conclusion was reached previously regarding the studies of neutron-irradiated Mo.[2] The magnitude of this dependence on temperature is weaker than has been predicted theoretically for trapping at voids.[1,11]

Another result of the fits to the data in Fig. 4 is that the trapping rate into shallow traps is very weak ($\lambda_2/\kappa_{12}\sim0.1$ means that $\kappa_{12}\sim6\times10^{10}$ sec^{-1})
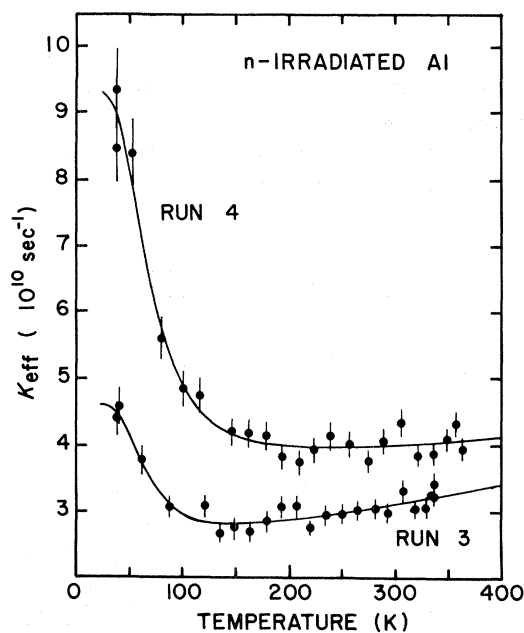
FIG. 4. The removal rate κ_{eff} of positrons from the free state is shown for the third and fourth runs as a function of sample temperature. The solid lines are the results of a nonlinear fit of the model described in the text to the data (parameters listed in Table I). The model is based on a temperature-dependent competition between the probability of positron localization in shallow traps, deeper traps including voids, and its freely diffusing Bloch state.

relative to that for vacancies ($\kappa_V \sim 5 \times 10^{14}$ sec^{-1}; Ref. 43). This result has been predicted by golden-rule calculations of the trapping rate associated with shallow traps. Assuming that λ_2 does not change, the decrease of λ_2/κ_{12} from runs three to four (Table I) indicates that the "trapping rate" into dislocations has increased. This is clearly illustrated in Fig. 4 as an increase in the shallow-trap effect, and is consistent with our earlier results for neutron-irradiated Mo.[2] At that time we attributed this effect to the recovery of some of the deeper traps contributing to the "τ_1" trap set.

It is expected that the radiation-induced defects would present a complex variety of shallow traps for positrons, with different characteristic temperatures for thermal desorption.[2,44] Because of the uncertainty associated with any model for the distribution of these traps, the fits to the data shown in Fig. 4 were obtained with a single characteristic temperature in order to maintain the maximum simplicity. The "S" shape that is most apparent in the theoretical curves in Fig. 5 is a result of assuming a single activation energy. This feature would be removed if the model were expanded to include several activation energies. In addition, we did not attempt to include positron "pipe" diffusion (D_2) in the shallow traps as discussed in the Appendix. The inclusion of a finite value for D_2 would tend to increase (slightly) the diffusion length at the very lowest temperatures, thereby increasing E_0. The lack of data at low temperatures prevents a serious estimation of the relative importance of each of these various processes.

Figure 5 shows $E_0(T)$ for the third and fourth data sets with the theoretically predicted curves based on the same parameters used in Fig. 4 (Table I). The fourth data set had lower values of E_0 than the third over the entire temperature range studied. This may be related to the annealing between runs required to remove sputtering damage, or to some systematic difference associated with a failure to identically relocate the sample after moving it to the sputtering position. Although the shift in scale is not completely understood, it does not alter the conclusions we have presented, since the general features predicted by the model of a low-temperature competition for positrons are consistently represented in both sets of data.

V. CONCLUSIONS

We have used a slow-positron beam to measure the fraction of Ps atoms emitted from the surface of a neutron-irradiated single crystal of Al. These measurements were performed as a function of sample temperature and incident beam energy, thus allowing a measurement of the dependence of positron diffusion on temperature. We find that the positron's diffusion is more restricted at low temperatures (< 125 K) than would be expected from considerations of scattering by conduction electrons, acoustical phonons, and impurities. These results reinforce previous conclusions[2] that some radiation-induced defects (other than voids) act as shallow traps of varying depth from which positrons can be desorbed with relatively little thermal energy. We have presented a model that incorporates a competition for freely diffusing positrons between trapping in voids and other radiation-induced defects, escape to the vacuum as Ps, and localization, with thermal desorption, in shallow traps.
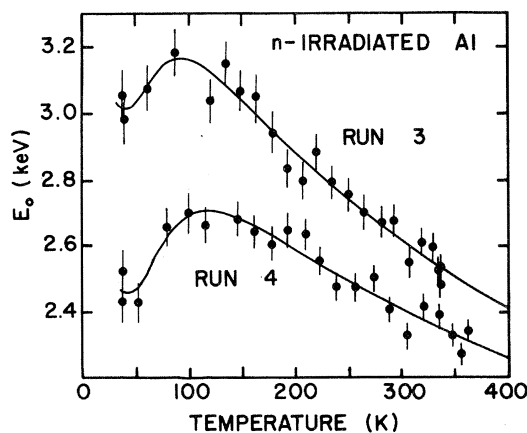
FIG. 5. E_0 is shown for the third and fourth runs as a function of sample temperature. The parameters used to generate the solid curves are the same as those used for Fig. 4. The turnover of E_0 below ~ 125 K is clear evidence for restricted positron diffusion. This is explained in terms of the localization of positrons in shallow traps.

ACKNOWLEDGMENTS

APPENDIX

The aim of this appendix is to present the essential assumptions underlying our interpretation of observed changes in the positronium fraction F as described in Sec. III, in terms of a particular pattern of positron trapping in the bulk aluminum metal. The analysis is divided into three main parts. In Sec. 1, we consider the dependence of F on incident positron energy E and the effective positron diffusion length L_+ in the bulk metal. Here we pay particular attention to the real situation in most experiments where the positron stopping or implantation profile is not precisely defined. In Sec. 2 we show when and how the treatment given in Sec. 1 can be realistically applied to a complicated pattern of positron trapping in the bulk by a rate-equation approach closely paralleling that frequently used in more conventional positron-trapping studies. Finally, in Sec. 3 we particularize to the problem of current interest by modeling the temperature dependence of L_+ that could result from competition between positron trapping in shallow traps and other more strongly trapping defect species.

1. The dependence of Ps fraction F on incident positron energy and bulk diffusion parameters

The Ps fraction F clearly depends on both surface and bulk phenomena. As long as the probability of nonthermal positron re-emission is small we may reasonably write $F = F_0 J(E)$, where $J(E)$ is the probability that a thermalized positron of initial energy E diffuses back to the surface and F_0 is the fraction of such positrons that eventually form Ps. We begin by considering $J(E)$ through the usual one-dimensional—diffusion picture. We assume that the implanted positrons all thermalize into freely diffusing states with an initial position distribution or stopping profile $P(x,E)dx$ within the metal $(x > 0)$. Since, in the experiments under discussion, the instantaneous positron density in the specimen is always vanishingly small (i.e., one positron) and the spectrum accumulations are made over periods long compared with the characteristic positron lifetimes involved, we may work in the steady-state limit.[29] Such an approach has considerable advantage because of its simplicity over the time-dependent analyses sometimes presented. In this limit, the time-independent density $n(x)$ of freely diffusing positrons in the specimen is determined by

$$D_+ \frac{\partial^2 n(x)}{\partial x^2} - \kappa_{\text{eff}} n(x) + P(x,E) = 0 , \qquad \text{(A1)}$$

where D_+ is the effective positron diffusion coefficient for the freely diffusing states and κ_{eff} is the total rate at which positrons are removed from those states by any process. In this derivation it is assumed that a homogeneous system exists in which both D_+ and κ_{eff} are independent of x. For convenience we also set $\int_0^\infty P(x,E)dx = 1$ throughout. The solution of Eq. (A1), well behaved within the metal $[n(x) \to 0$ as $x \to \infty]$, is

$$n(x) = Ce^{-\beta x} + \frac{1}{2\beta D_+} \int_0^\infty e^{-\beta |x-x'|} P(x',E)dx' .$$

$$\text{(A2)}$$

$\beta = L_+^{-1} = (\kappa_{\text{eff}}/D_+)^{1/2}$ is the characteristic positron inverse diffusion length within the metal and C is a constant to be determined by the further boundary conditions at the surface $x = 0$. We adopt the usual radiative condition[22] in which the emerging positron flux is

$$J(\beta,E) = vn(0) = D_+ \frac{\partial n(x)}{\partial x} \bigg|_{x=0^+} \qquad \text{(A3)}$$

Here v is determined by the actual surface physics. In the case of a perfectly absorbing boundary $v \to \infty$ as $n(0) \to 0$. Application of condition (A3) to the $n(x)$ of expression (A2) then yields the well-known result

$$J(\beta,E) = (1 + \beta D_+ /v)^{-1} \int_0^\infty e^{-\beta x} P(x,E)dx$$

$$\text{(A4)}$$

in which the E dependence of J is entirely and simply determined by the Laplace transform of $P(x,E)$. The dependence of J on the positron diffusion parameters enters both via this transform and the "transmission coefficient" $(1 + \beta D_+ /v)^{-1}$. However, in any situation in which E is the only varying parameter we can absorb this coefficient into the original surface parameter F_0 which appeared in our starting equation for F, $F = F_0 J(E)$. Then, if, irrespective of its general form, $P(x,E) \to \delta(0)$ as $E \to 0$, we may write

$$F = F_0 \int_0^\infty e^{-\beta x} P(x,E)dx = F_0 L(\beta,E) , \qquad \text{(A5)}$$

where F_0 is the Ps fraction at $E=0$. It remains for us to establish the form of $L(\beta,E)$.

If $P(x,E)=x_E^{-1}\exp(-x/x_E)$, then $L(\beta,E)=(1+\beta x_E)^{-1}$. Then, if $\bar{x}_E=AE^n$ where A is a constant, as is generally the case for the measured, albeit variously defined, stopping depths for low-energy electrons, then

$$F=F_0[1+(E/E_0)^n]^{-1} , \qquad (A6)$$

where $\beta^{-1}=L_+=AE_0^n$. This prescription for F, with values of n varying from 1 to 1.6, has been used in several earlier works notwithstanding the fact that both electron[46] and positron[47] stopping studies suggest profiles that deviate from the exponential form. However, a wider justification for the use of this simple form is not hard to find. Whenever the profile can be so described it is easy to show from Eq. (A5) that $L(\beta,E)=L(\beta x_E)=L(E/E_0)$. Further, since we always have freedom to vary the definition of $\bar{x}_E$ to the extent of an arbitrary multiplicative constant, we can arrange, in addition to the necessary $L(0)=1$ and $L(\infty)=0$, that $L(1)=0.5$. This done, then at least for the range $0.25 \lesssim (E/E_0) \lesssim 2.5$ and the present level of statistical precision in F (see Sec. III), Eq. (A6) can adequately deal with all plausible forms $P(x/x_E)$. This is true so long as n is simply regarded as a parameter of the fit and not a precise description of a power-law relation between some particularly defined positron range and E. Although, at the present levels of experimental precision, we cannot expect to establish the detailed form of $P(x,E)$ through observations of the dependence of F on E, we can at least study positron behavior in the bulk through the reciprocal dependence on E_0 and related diffusion parameters.

2. The positron diffusion length L_+: A trapping-model analysis

In a structurally perfect pure metal crystal we could anticipate that $D_+ \sim 1$ cm^2 sec^{-1} varying as $T^{-1/2}$,[12] and κ_{eff} [Eq. (A1)]$=\lambda_f$, the reciprocal bulk positron lifetime $\sim 10^{10}$ sec^{-1}. The extension to a defected system containing a variety of potential positron traps can be straightforwardly made via the usual trapping-model approach. Following the notation of Ref. 32, and with an obvious generalization of that of Eq. (A1), we write

$$D_{+,i}\frac{\partial^2 n_i}{\partial x^2}(x)-\left[\lambda_i+\sum_{J\neq 1}^{N}\kappa_{i,j}\right]n_i(x)$$
$$+\sum_{j\neq 1}^{N}\kappa_{i,j}n_j(x)+P_i(x,E)=0 \qquad (A7)$$

for all N supposed distinguishable positron states (i). Simple addition of all N equations (A7) then yields a single equation like (A1) in which the explicit dependence on all the various transition rates $\kappa_{i,j}$ is removed but replaced by an implicit dependence through a D_+ and κ_{eff} which are complicated averages involving the individual $D_{+,i}$ and λ_i, and the $n_i(x)$ or their second derivatives. In principle, this is ultimately the sense in which D_+ and κ_{eff} must always be regarded. Further D_+ and κ_{eff}, thus defined, will, in general, be functions of x as in the more general case when the system is intrinsically inhomogeneous. The resultant complexity of the problem then rules out realistic analysis.

A more rewarding state of affairs results from three simple assumptions. We assume as is usual in such analyses that all the positrons thermalize into a single freely diffusing state $i=1$, i.e., $P_i(x,E)=P_i(x,E)\delta_{i,1}$, and that all the $\kappa_{i,j}$ are zero unless one or other of i and j are 1. Both these assumptions are consistent with contemporary pictures of positron-trapping phenomena. We further assume that diffusion in all the secondary ($i\neq 1$) states can be neglected, i.e., $D_{+,i}$ ($i\neq 1$)$=0$. This final assumption is more fragile but is considered further in Sec. IV. Then for all the secondary states, Eq. (A7) becomes $(\lambda_i+\kappa_{i,1})n_i(x)=\kappa_{1,i}n_1(x)$, which, when inserted in the remaining equation for $i=1$, yields Eq. (A1) but with $n(x)=n_1(x)$, $D_{+,i}=D_{+,1}$, and

$$\kappa_{\text{eff}}=\lambda_1+\sum_{i\neq 1}^{N}\kappa_{1,i}\lambda_i(\lambda_i+\kappa_{i,1})^{-1} . \qquad (A8)$$

Since only those positrons in state 1 are free to diffuse to the surface, we have reduced our problem to that already dealt with in Sec. 1. It only remains for us to model the κ's and λ's.

3. Shallow positron traps

In response to the results presented in Sec. IV we now consider a system in which the various defects or trapping centers implied in Eq. (A8) can be clearly divided into two classes: (a) shallow

traps, henceforth denoted by $i = 2$, for which both κ_{12} and κ_{21} are comparable with each other, and with λ_2, at least for some attainable temperature range, and (b) deeper traps for which the $\kappa_{i,1}$ can always be neglected as compared with the corresponding λ_i. Then,

$$\kappa_{\text{eff}} = \lambda_1 + \sum_{i \neq 1,2}^{N} \kappa_{1,i} + \kappa_{12}\lambda_2(\lambda_2 + \kappa_{21})^{-1} . \quad \text{(A9)}$$

Our primary interest is the temperature dependence of the final term in Eq. (A9) which we model via an analysis which closely parallels that recently given by Smedskjaer et al.[48]

We assume that the freely diffusing states $i = 1$ lie within a parabolic conduction band wtih a density of available states in energy $g(\epsilon) = 8\sqrt{2}\pi h^{-3} \times (m^*)^{3/2}\epsilon^{1/2}$ per unit volume. Here m^* is the positron band effective mass and h is Planck's constant. The shallow-trap states are strongly peaked around an energy $-\epsilon_0$, somewhere below the conduction band edge ($\epsilon = 0$) and arise from a weak

positron localization around centers of spatial density N_0 per unit volume. From our analysis in Sec. 2 we have that $\kappa_{12}n_1 - (\lambda_2 + \kappa_{21})n_2$. In the limit that $\lambda_2 \ll \kappa_{21}$, and thermodynamic equilibrium, defined by the nondegenerate classical limit of the Fermi-Dirac distribution $\exp[(\mu - \epsilon)/k_B]$, exists, we may deduce that

$$\frac{\kappa_{21}}{\kappa_{12}} = \frac{n_1}{n_2} = \int_0^{\infty} e^{(\mu-\epsilon)/k_B} g(\epsilon) d\epsilon / e^{(\mu+\epsilon_0)/k_B} N_0$$

$$= 2 \left[\frac{2\pi m^* k_B T}{h^2} \right]^{3/2} e^{-\epsilon_0/k_B} N_0^{-1} . \quad \text{(A10)}$$

Since the overall positron density is so small ($n \leq V^{-1}$ where V is the sample volume) we would argue that this expression for κ_{12}/κ_{21} must remain valid for finite λ_2. Then, if $\kappa_{12} = N_0 \Gamma_0(T)$—we refrain from choosing a particular form for $\Gamma_0(T)$ since the trapping centers in question remain undefined—we may rewrite Eq. (A9) as

$$\kappa_{\text{eff}}(T) = \lambda_1(T) + \sum_{i \neq 1,2}^{N} \kappa_{1,i}(T) + \lambda_2(T) \left[\frac{\lambda_2(T)}{N_0 \Gamma_0(T)} + \frac{2}{N_0} \left[\frac{2\pi m^* kT}{h^2} \right]^{3/2} e^{-\epsilon_0/kT} \right]^{-1} . \quad \text{(A11)}$$

The application of this result is discussed in Sec. IV.

*Visiting from the Physics Department, University of Guelph, Guelph, Ontario N1G 2W1, Canada.

†Visiting from School of Mathematics and Physics, University of East Anglia, Norwich, England.

‡Present address: Technology for Energy Corp. Knoxville, Tennessee 37922.

[1]R. M. Nieminen, J. Laakkonen, P. Hautojärvi, and A. Vehanen, Phys. Rev. B **19**, 1397 (1979).

[2]P. J. Schultz, K. G. Lynn, I. K. MacKenzie, Y. C. Jean, and C. L. Snead, Jr., Phys. Rev. Lett. **44**, 1629 (1980); C. L. Snead, Jr., K. G. Lynn, Y. Jean, F. W. Wiffen, and P. Schultz, J. Nucl. Mater. (in press).

[3]P. C. Lichtenberger, C. W. Schulte, and I. K. MacKenzie, in the Proceedings of the 4th International Conference on Positron Annihilation, Helsingor, 1976 paper E25, (unpublished).

[4]I. K. MacKenzie, Phys. Rev. B **16**, 4705 (1977).

[5]M. Eldrup, B. T. A. McKee, and A. T. Stewart, J. Phys. F **9**, 637 (1979).

[6]Lars C. Smedskjaer, Matti Manninen, and Michael J. Fluss, J. Phys. F **10**, 2237 (1980).

[7]A. P. Mills, Jr., Phys. Rev. Lett. **41**, 1828 (1978).

[8]K. G. Lynn, J. Phys. C **12**, L435 (1979).

[9]I. J. Rosenberg, A. H. Weiss, and K. F. Canter, in the Proceedings of the 26th National Symposium of the American Vacuum Society, 1979 (unpublished).

[10]A. Seeger, Phys. Lett. **40A**, 135 (1972).

[11]W. Brandt, Appl. Phys. **5**, 1 (1974).

[12]B. Bergersen, E. Pajanne, P. Kubica, M. J. Stott, and C. H. Hodges, Solid State Commun. **15**, 1377 (1974).

[13]A. Alam, P. Fellows, J. D. McGervey, and R. N. West, Radiat. Eff. **50**, 27 (1979).

[14]S. Mantl, W. Kesternich, and W. Triftshäuser, J. Nucl. Mater. **69/70**, 593 (1978).

[15]R. W. Hendricks, J. Schelten, and W. Schmatz, Philos. Mag. **30**, 819 (1974).

[16]J. E. Epperson, R. W. Hendricks, and K. Farrell, Philos. Mag. **30**, 803 (1974).

[17]V. W. Lindberg, J. D. McGervey, R. W. Hendricks, and W. Triftshäuser, Philos. Mag. **36**, 117 (1977).

[18]R. W. Hendricks, J. Schelten, and G. Lippman, Philos. Mag. **36**, 907 (1977).

[19]R. Bullough and A. B. Lidiard, Comments Solid State Phys. **4**, 69 (1972).

[20]A. Seeger, Comments Solid State Phys. **4**, 79 (1972).

[21]K. Farrell, J. Bentley, and D. N. Braski, Scr. Metall. **11**, 243 (1977).

[22]K. G. Lynn and H. Lutz, Rev. Sci. Instrum. **51**, 977 (1980).

[23]K. G. Lynn and D. O. Welch, Phys. Rev. B **22**, 99 (1980).

[24]See, for example, the review by R. N. West, Adv. Phys. **22**, 263 (1973).

[25]Allen P. Mills, Jr., Solid State Commun. **31**, 623 (1979).

[26]K. G. Lynn, Phys. Rev. Lett. **43**, 391 (1979).

[27]A. P. Mills, Jr., P. M. Platzman, and B. L. Brown, Phys. Rev. Lett. **41**, 1076 (1978).

[28]K. G. Lynn and H. Lutz, Bull. Am. Phys. Soc. **24**, 271 (1979).

[29]H. J. Kreuzer, D. N. Lowy, and Z. W. Gortel, Solid State Commun. **35**, 381 (1980).

[30]A. Ore and J. L. Powell, Phys. Rev. **75**, 1696 (1949).

[31]Joseph Callaway, Phys. Rev. **116**, 1140 (1959); A. Held and S. Kahana, Can. J. Phys. **42**, 1908 (1964); D. N. Lowy and A. D. Jackson, Phys. Rev. B **12**, 1689 (1975).

[32]*Positron in Solids*, edited by P. Hautojärvi (Springer, New York, 1979); in particular, R. N. West's contribution.

[33]K. G. Lynn and H. Lutz, Phys. Rev. B **22**, 4143

[34]K. G. Lynn, P. J. Schultz, and I. K. MacKenzie, Solid State Commun. **38**, 473 (1981).

[35]W. Shockley and J. Bardeen, Phys. Rev. **77**, 407 (1950).

[36]J. Bardeen and W. Shockley, Phys. Rev. **80**, 72 (1950).

[37]E. M. Conwell, *Solid State Physics* (Academic, New York, 1967), Suppl. 9.

[38]A. P. Mills, Jr., Proceedings of the 83rd Session of the International School of Physics "Enrico Fermi," 2nd Course, Varenna, Italy, 1981 (unpublished).

[39]P. Kubica, Ph.D thesis, Queens University, 1975 (unpublished).

[40]C. Kittel, *Introduction to Solid State Physics*, 5th ed., (Wiley, New York, 1976).

[41]Handbook of Auger Electron Spectroscopy, Physical Electronics (unpublished).

[42]Neil W. Ashcroft and N. David Mermin, *Solid State Physics* (Holt, Rinehart and Winston, New York, 1976).

[43]R. M. Nieminen and J. Laakkonen, Appl. Phys. **20**, 181 (1979).

[44]H. E. Hjelmroth, J. G. Rasmussen, and J. Träff, Nuovo Cimento B **41**, 284 (1977).

[45]Thomas M. Hall, A. N. Goland, and C. L. Snead, Jr., Phys. Rev. B **10**, 3062 (1974).

[46]A. F. Makhov, Fiz. Tverd. Tela (Leningrad) **2**, 2161 (1960) [Sov. Phys.—Solid State **2**, 1934 (1960)].

[47]R. J. Wilson and A. P. Mills, Jr., (unpublished).

[48]L. C. Smedskjaer, Matti Manninen and Michael J. Fluss, J. Phys. F **10**, 2237 (1980).

(1980).